ANN MODELLING OF CORROSION INHIBITION OF MILD STEEL IN MARINE ENVIRONMENT USING EPOXY-NICKEL OXIDE NANOCOMPOSITE COATINGS

Kooffreh Okon[*1,2]Ifeyinwa Calista Ekeke[1], Chidiebere Arinzechukwu Maduabuchi[1], Ikechukwu Ignatius Ayogu[1], Taofik Oladimeji Azeez[1], Christogonus Oudney Akalezi[1]

[1]*Africa Centre of Excellence in Future Energies and Electrochemical Systems, Federal University of Technology, PMB 1526 Owerri (ACE-FUELS, FUTO), Imo State, Nigeria.*

[2]*Department of Materials and Metallurgical Engineering, Federal University of Technology, PMB 1526 Owerri, Imo State, Nigeria.*

[*]*Corresponding Author Email address: koofsco1@gmail.com*

AJME 2025, 23 (2); https://doi.org/10.5281/zenodo.15863489

ABSTRACT: *The corrosion inhibition of mild steel in 3.5 wt. % NaCl in the absence and presence of epoxy coatings containing varying concentration of Nickel oxide nanoparticles was studied using the gravimetric technique within the operating temperature range of 30 to 60oC. A predictive model based on the Artificial Neural Network (ANN) was developed to study the relationship between the input variables (exposure time, inhibitor concentration and Temperature) and output variables (Corrosion Rate and Inhibition Efficiency). The ANN model was based on the Multilayer Perceptron algorithm with input layer comprising of 23 units and 1 hidden layer consisting of 3 units. Corrosion test data obtained from 80 experimental runs were successfully modelled using ANN with minimal errors. 56 cases corresponding to 70% of test data were used for training the network and 24 cases corresponding to 30% of test data was used for testing the efficacy of the network.*

KEYWORDS: *ANN, Nickel Oxide Nanoparticles, Epoxy resin, Mild Steel, Corrosion Inhibitors*

1 INTRODUCTION

Corrosion of pipelines and other engineering infrastructure made from mild steel is a global problem and constitutes major economic and environmental losses to the oil and gas industries, chemical processing industries, food processing industries and desalination plants operating within the marine environment. Corrosion which is the gradual removal of the material surface due to interaction with its environment is an electrochemical process[1] and accounts for losses of about 3-5% of the world's GDP annually[2]. Development of strategies such as the use of protective coatings, inhibitors, cathodic protection, anodic protection, pigging of pipelines, appropriate materials selection and design to combat this menace has been the subject of many research efforts[3]–[6]. The use of corrosion inhibitors is very common among researchers due to their availability, low-cost, ease of use and environmental compatibility[7], [8]. Among the corrosion inhibitors used successfully in the past, plant extracts have been the most reported in literature. However, these extracts have the challenges of need for constant replacement and tendency to be carried away by corrosive fluid or leached into solution. The ability of metal oxide nanoparticles to overcome the aforementioned limitations has increased their demand as corrosion inhibitors and several metal oxide nanoparticles such as titanium oxide[9], nickel oxide[10], zinc oxide[11], silver oxide[12] have been used successfully as corrosion inhibitors. Nickel oxide nanoparticles is of particular interest due to its unique combination of hardness, high surface area to volume ratio, longevity, chemical and thermal stability in aggressive salt environments and synergistic effect with other corrosion inhibitors[13]–[15]. The efficacy of 3-Mercaptopropyl triethoxysilane (MPTES)-modified NiO nanoparticles in varying concentrations ranging from 1 to 3% embedded in epoxy resin as a corrosion inhibitor for mild steel in sea water was studied by using electrochemical impedance spectroscopy (EIS) and scanning electrochemical microscopy (SECM). Findings from the study revealed that the introduction of NiO nanoparticle in the epoxy coating enhances the charge transfer resistance (Rct) as well as the film resistance (Rf).

Epoxy-MPTES modified NiO nanocomposite coated steel significantly enhanced protective capacity of epoxy resin by preventing the transportation of H2O, O2 and corrosive ions into the epoxy resin and lowered the chances of degradation and blistering of the coating film[16]. The potential of epoxy/1.8 ZnO-NiO as an effective inhibitor for corrosion protection of steel in 3.5wt. % NaCl environment was studied using electrochemical impedance spectroscopy (EIS) and Potentiodynamic Polarization (PDP) measurements. Results from the electrochemical testing confirmed that improved anticorrosion performance was exhibited by the EP/1.8 ZnO-NiO–epoxy coating compared to the pure epoxy, EP/1 ZnO-NiO coatings due to the higher charge and resistance for the epoxy/1.8–ZnO-NiO nanocomposite coated steel[17]. In an attempt to produce more environmentally benign corrosion inhibitor, sustainable vegetable (soy) oil-based epoxy polymer blends (ESODG), and their nickel oxide (NiO) based organic-inorganic hybrid (ESODG-PA-NiO) nanocomposites were formulated as anticorrosive coatings. Addition of small amount of NiO nanoparticle in epoxy blend remarkably improved the hydrophobic characteristics, corrosion inhibition, metal surface adhesion, scratch hardness, and abrasion resistance properties of the hybrid composite coatings. The excellent anticorrosive performance of ESODG- PA-NiO hybrid was attributed to the electrostatic interaction between NiO and ESODG-PA, which provide additional locking/sealing effect and rectified polymeric artifacts and can be used as a surface decorative/ protective anticorrosive coating[18]. Corrosion is a complex process with many variables at play at the same time[19]. Mathematical modelling is used to study the contribution of each of the process variables to the entire corrosion process[20]. In this study, NiO nanoparticles prepared by chemical precipitation technique were embedded in epoxy resin and used as nanocomposite coatings for corrosion inhibition of mild steel in 3.5 wt. % NaCl at different operating conditions. Corrosion rate and inhibition efficiency were monitored using weight loss technique in absence and presence nanoscale NiO with epoxy coating. The relationship between process parameters including exposure time, temperature and inhibitor concentration were correlated using ANN modelling of test data.

2 METHODOLOGY

2.1 Metal Preparation and Procedure

Mild Steel with dimensions of 2 cm x 3 cm x 0.2 cm and total surface area of about 14 cm2 was used as the working electrode. The composition of the mild steel used is tabulated in table 1.

Table 1: Chemical composition of mild steel

Element	C	Mn	P	Si	S	Cu	N	Cr	Fe
Composition (wt. %)	0.14	0.48	0.017	0.18	0.005	0.03	0.007	0.79	98.43

Before use, the specimens were degreased with acetone and abraded sequentially with emery papers ranging from 220 to 1200 grades. This was closely followed by rinsing with running water, drying and rinsing with acetone. The cleaned specimens were preserved in a desiccator over silica gel until they were ready to be used for experiments. The blank specimen, pristine epoxy coated specimen and specimens coated with epoxy resin containing varying concentrations of 1, 2, 3 and 5 wt. % NiO respectively were completely submerged in 400cm3 of 3.5 wt. % NaCl for a duration of 60 days at intervals of 5 days at room temperature(25oC). Subsequently, the specimens were submerged in 250cm3 of 3.5 wt. % NaCl for a duration of 5 hours in the absence and presence of epoxy resin and the nanocomposite coatings at temperatures of 30, 40 and 60oC respectively. The specimens were thoroughly washed with water after each experiment, dried with cotton wool, rinsed with acetone, dried with a hand dryer and subsequently weighed with a high precision electronic analytical weighing balance.

2.2 Synthesis of Nickel Oxide Nanoparticles

Pure solid nickel crucible was dissolved in 330ml of 12M concentrated Hydrochloric acid (HCl) containing 37% wt. % HCl to form nickel chloride in aqueous solution accompanied by the liberation of hydrogen gas according to the reaction:

$$Ni(s) + 2HCl\ (aq) \rightarrow NiCl_2 + H_2\ (g) \quad (1)$$

The conversion of nickel chloride (NiCl2) into nickel oxide (NiO) was achieved by titrating the nickel chloride against 2M NaOH solution obtained by dissolving 80g of NaOH pellets in 1litre of distilled water which resulted in the precipitation of nickel hydroxide Ni(OH)2 as a green solid according to the reaction:

$$NiCl_2\ (aq.) + 2NaOH\ (aq.) \rightarrow Ni(OH)_2\ (s) + 2NaCl\ (aq.) \quad (2)$$

The green precipitate of Ni(OH)2 was filtered and washed several times, dried in air and subsequently converted into nickel oxide (NiO) through a heating process by calcination for three hours in a muffle furnace at a temperature of about 300oC. The reaction below represents the dehydration of nickel hydroxide to form nickel oxide and water vapour.

$$Ni(OH)_2\ (s) \rightarrow NiO\ (s) + H_2O\ (g) \quad (3)$$

2.3 Characterization of Nickel Oxide Nanoparticles

The characterization of the synthesized NiO nanoparticles was done using a combination of XRD and SEM-EDX techniques. Structural analysis was performed using Thermo Scientific ARL X'TRA X-ray Diffractometer (XRD) with serial number 197492086, a product of Thermo fisher Scientific Company Switzerland. The elemental composition of the synthesized nanoparticles was studied using the JEOL JSM 7600F Scanning Electron Microscope.

2.4 Preparation and Application of Coatings on mild steel specimens

The coatings for the mild steel specimens were produced by mixing epoxy resin based on diglycidyl ether of bisphenol A (DGEBA) with an amine hardener, tetraethylenepentamine (TEPA) in the ratio of 2: 1 by weight. Varying concentrations of 1, 2, 3 and 5 wt. % NiO were added to the coating mixture and the contents were mechanically stirred for about 30 minutes and ultrasonicated for about 15 minutes for homogenization. Well cleaned mild steel specimens suspended by polymeric threads were fully dipped into the coating mixture and subsequently sun dried for 48 hours for full curing.

2.5 Characterization of coatings

The presence of epoxy resin, tetraethylenepentamine hardener and nickel oxide nanoparticles in the coating mixture were detected using Fourier Transform Infrared Spectroscopy, FTIR [PerkinElmer Instrument, Spectrum Two FT-IR Spectrometer (LiTaO3 Detector) with serial number 122344].

2.6 Corrosion Rate Measurements

The corrosion inhibition data for mild steel in the presence and absence of epoxy-nickel oxide nanoparticles for 60 days of immersion in 3.5wt % NaCl was obtained using the gravimetric method. Corrosion rate was calculated using the formula:

$$CR = \frac{Weight\ loss\ (g)}{Area\ (m^2)\ X\ Time\ (day)} \quad (4)$$

Where CR is the Corrosion rate in gm-2day-1.

While the corrosion inhibition efficiency was calculated using the formula:

$$\%\ IE = \frac{CR^0 - CR^i}{CR^0}\ X\ 100 \quad (5)$$

Where % IE = percentage inhibition efficiency, CR^0 = Corrosion rate of uncoated sample,

CR^i= Corrosion rate of coated sample.

2.7 Development of ANN Model for Corrosion Test Data

Artificial Neural Network (ANN) modelling of corrosion test data was carried out using the neural network tool of IBM SPSS Statistics version 27 software. The Multilayer Perceptron algorithm was adopted for this study for the modelling of data obtained from 80 experimental runs with 56 cases constituting 70% of test data used for training the network and 24 cases corresponding to 30% of test data was used for testing the efficacy of the network. The independent (input) variables used were inhibitor concentration (wt. % NiO), exposure time (hr) and temperature(oC) while the dependent (output) variables were corrosion rate(g/m2/day) and inhibition efficiency (%). The input layer consisted of 23 units while the hidden layer consisted of 3 units with hyperbolic tangent as its activation function. The output layer contained 2 units with standardized rescaling method for scale dependents, identity activation function and sum of squares adopted as the error function.

2.8 Measurement of Error In Prediction

The extent of closeness between the actual experimental values obtained and the predicted values from ANN modelling of experimental data can be evaluated using the Mean Absolute Error (MAE) and Mean Square Error (MSE)[21]. Mathematically, the Mean Square Error can be computed using the relationship in equations 8 and 9 respectively.

$$MAE = \frac{1}{n}\sum_{i=1}^{n}|f_i - y_i| \quad (8)$$

Where n = number of samples, $f_i = the\ predicted\ value, y_i = the\ true\ value$

$$MSE = \frac{1}{N}\sum(f_i - y_i)^2 \quad (9)$$

Where N = number of samples, $f_i = an\ estimator\ of\ parameter, y_i$ and $y_i = the\ true\ value$

3 RESULTS AND DISCUSSION

3.1 Structural Analysis of NiO NPs

The X-ray diffraction pattern for the synthesized nickel oxide nanoparticles is shown in figure 1.

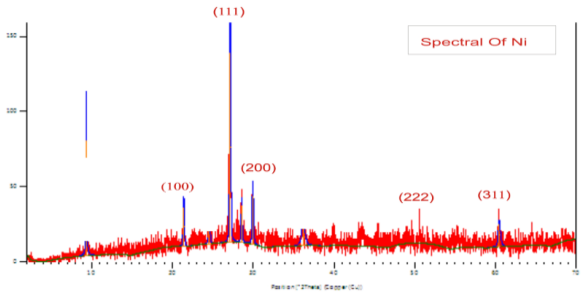

Figure 1: XRD Analysis of synthesized nickel oxide nanoparticles

The (100), (111), (200), (222) and (311) planes corresponding to diffraction angles of 21.5o, 27.5o, 30.7o, 51o and 60.9o respectively detected at major diffraction peaks confirmed the synthesis of nickel oxide with a lattice constant of 4.1749Å (DB Card number 01-076-6122). The average crystallite size was calculated to be about 23nm using the Debye-Scherrer formula[22] which is given as:

$$D = \frac{Shape\ factor\ X\ x{-}ray\ wavelength}{Full\ width\ at\ half\ maximum, FWMH\ X\ Cos\theta} \quad (1)$$

3.2 Compositional Analysis of NiO NPs

The EDX pattern of the synthesized nickel oxide nanoparticles shown in figure 2 revealed that the composition of the sample is made up of 67.89% Ni and 10.14% O with a small concentration of other elements such as C, Cu, Zr, Fe, S and K with composition of 3.65% C, 4.70%, 4.10%, 3.70%, 2.62% and 3.20% respectively. The presence of Carbon can be attributed to the residue formed from the calcination process while the presence of other elements can be attributed to contamination from the crucible or possibly reagents used for the synthesis.

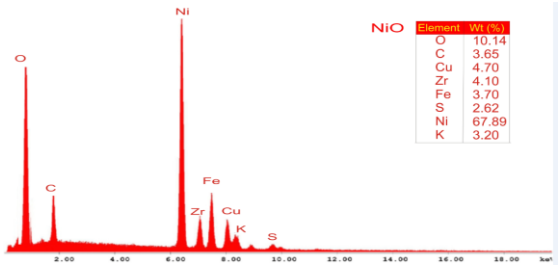

Figure 2: EDX Analysis for synthesized nickel oxide nanoparticles

3.3 Characterization of Coating mixture

The FTIR spectra for the epoxy resin, hardener and nanocomposite coating are shown in figure 3.

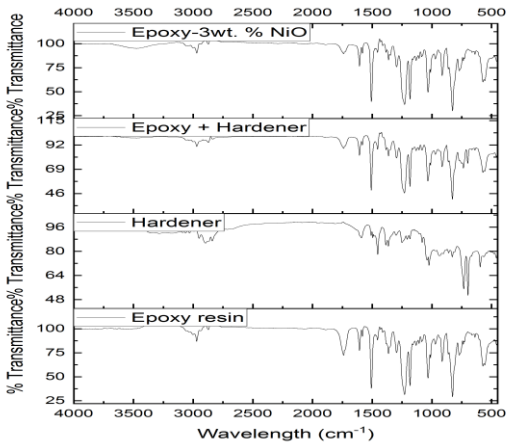

Figure 3: FTIR spectrum of coating mixture

For epoxy resin, the peaks observed within the range 2970.71 to 2872.83cm-1 were assigned to Stretching of C-H of CH2 and CH aromatic and aliphatic chains[23] while the peak bands observed at 1738.52 to 1607cm-1 were assigned to the Stretching C=C of aromatic rings. Other peaks detected at 1581.93cm-1, 1032.33cm-1, 914.31cm-1, 827.07cm-1 and 770.84cm-1 were attributed to the occurrence of Stretching of C-C of aromatic, Stretching of C-O-C of ethers, Stretching of C-O of oxirane group, Stretching of C-O-C of oxirane group and Rocking of CH2 respectively[23], [24]. For the hardener, observed peaks at 3284.25 cm-1; 2949.70 – 2896.12 cm-1; 1591.20 cm-1; 1453.12 cm-1; 1207.25 cm-1; 1039.52 cm-1; 732.75 – 594.87 cm-1; 459.45 cm-1 were attributed to the occurrence of N-H stretching of amines or amides; C-H stretching vibration; C=C aromatic bending or stretching; C-H bending; C-N stretching; C-O stretching; C-H out of plane bending and Metal-ligand bending respectively[25], [26]. The NiO nanoparticles had peaks at 3350cm-1 and 1624 cm-1 due to the presence of Oxygen-Hydrogen bonding[27]. Other peaks observed at 944 cm-1 and 579 cm-1 were assigned to Nickel-Oxygen Tetrahedral Bonding and Metal-Oxygen stretching respectively[13], [27].

3.4 Corrosion Rate

The results of the gravimetric measurements illustrated in figures 4 and 5 give a summary of the corrosion rate and percentage inhibition efficiency of uncoated and coated mild steel samples with epoxy resin containing varying concentrations of nickel oxide nanoparticles immersed in 3.5wt % NaCl for 60 days at room temperature.

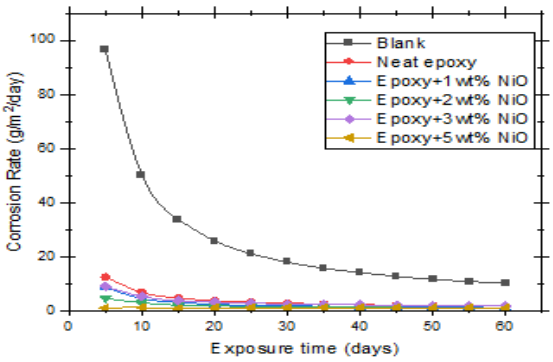

Figure 4: Corrosion rate of blank and coated mild steel in 3.5 wt % NaCl

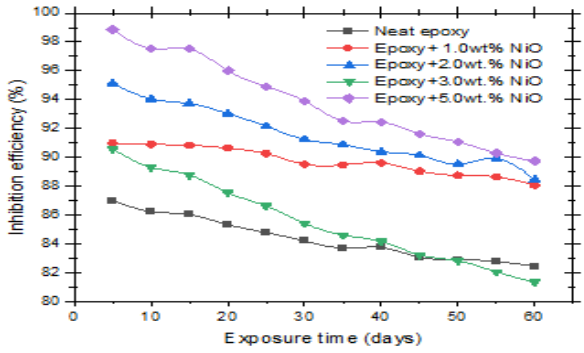

Figure 5: Inhibition efficiency of blank and coated mild steel in 3.5 wt % NaCl

Epoxy-5wt% nickel oxide inhibitor concentration produced the best inhibitive effect. The resistance to corrosion process exhibited by the epoxy-nickel oxide nanocomposites can be explained in terms of the ability of the inhibitor to get adsorbed at the reaction sites (cathode and anode) on the metal surface by blocking the metal pores and forming a thin layer thereby preventing the free flow of electrons for corrosion reactions[28]. The corrosion resistance is also enhanced by the excellent barrier property of epoxy resin as well as the polar functional groups present in epoxy resin which serve as adsorption sites to the metal substrate[17], [29]. It can be seen from figure 5 that the inhibition efficiency generally increases with an increase in the wt. % of NiO in the epoxy-nickel oxide nanocomposite coatings but decreases with prolonged exposure time. This can be attributed to prolonged exposure to saline conditions, stress, moisture, mechanical wear, leaching of nanoparticles into the solution, loss of contact of nanoparticles with the substrate and possible delamination which can compromise the protective properties of the coatings.

3.5 Effect of Temperature

It is evident from figures 6 and 7 that the increase in temperature significantly increased the corrosion rates of the coated and uncoated samples and reduced the percentage inhibition efficiency. The effect of temperature on corrosion rate is governed by an Arrhenius type relationship[30] (equation 8). Epoxy coated Mild steel samples immersed in 3.5 wt. % NaCl exhibited the least percentage inhibition efficiencies of 24.29%, 25.97% and 23.55% at temperatures of 30oC, 40oC and 60oC respectively while Mild steel samples coated with Epoxy- 5 wt. % NiO had the highest percentage inhibition efficiency values of 81.07%, 78.54% and 70.39% at temperatures of 30oC, 40oC and 60oC respectively as illustrated in figure 10 due to the enhanced corrosion resistance induced by the presence of Nickel oxide nanoparticles in epoxy resin.

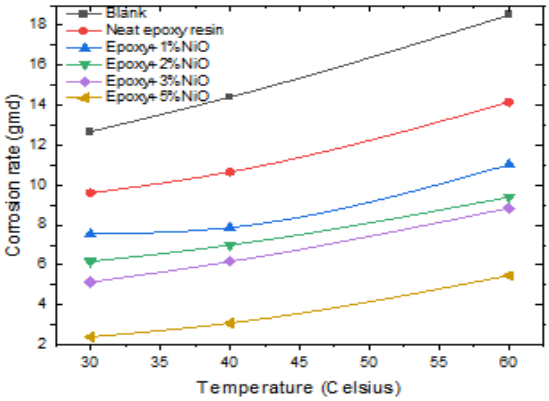

Figure 6: Effect of Temperature on corrosion rate

$$CR = A \exp\left(-\frac{E_a}{RT}\right) \quad (8)$$

Where CR is the corrosion rate, R is the universal gas constant, T is the absolute temperature and A is a pre-exponential factor.

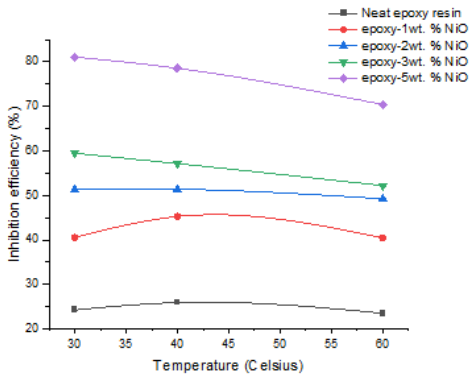

Figure 7: Effect of Temperature on Inhibition efficiency

3.6 Surface Roughness Analysis

The surface roughness values obtained from AFM Characterization of selected samples after 60 days of immersion in 3.5wt. % NaCl are presented in table 2 while the AFM micrographs are illustrated in figures 8 to 11. The progressive reduction of surface roughness values from the blank with average value of 0.1854 to the pure

epoxy coated mild steel with average value of 0.1206 and subsequently to the epoxy-NiO nanocomposite coatings containing 1.0 and 3.0 wt. % NiO with average values of 0.1047 and 0.0452 respectively confirm that the corrosion rate is reduced as the concentration of NiO is increased in the epoxy resin.

Table 2: Surface Roughness values of selected samples

Sample	Average value	RMS roughness (Sq)	RMS (grainwise)	Mean roughness (Sa)	Maximum Peak height(Sp)	Maximum Peak depth(Sv)	Maximum height (Sz)
Blank	0.1854	0.07872	0.07872	0.04283	0.8146	0.1854	1.0000
Epoxy coated MS	0.1206	0.05295	0.05295	0.02655	0.8794	0.1206	1.0000
Epoxy-1wt% NiO coated MS	0.1047	0.1432	0.1432	0.0919	0.8953	0.1047	1.0000
Epoxy-3wt% NiO coated MS	0.0452	0.06408	0.06408	0.03146	0.9548	0.0452	1.0000

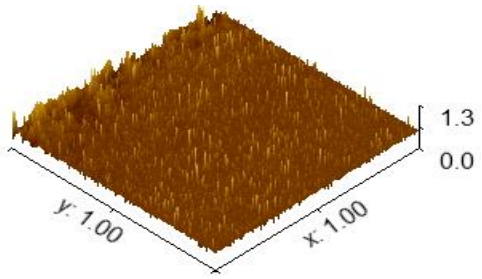

Figure 8: 3-D AFM micrograph of blank sample in 3.5 wt.% NaCl

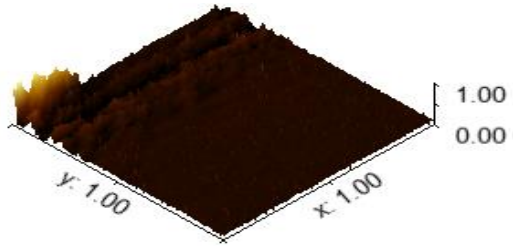

Figure 9: AFM image of epoxy resin coated sample in 3.5 wt.% NaCl

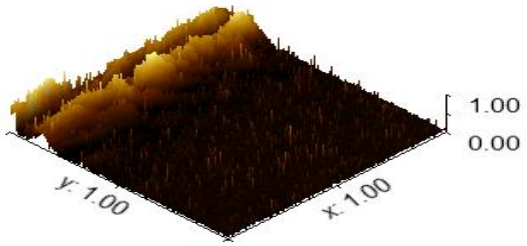

Figure 10: AFM image of epoxy-1.0 wt. % NiO coated sample in 3.5 wt.% NaCl

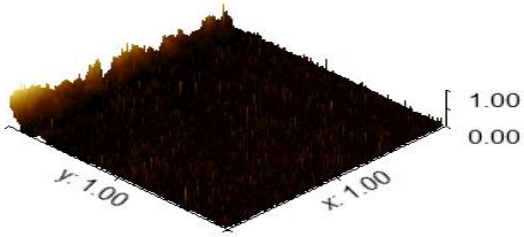

Figure 11: AFM micrograph of epoxy-.3.0 wt. % NiO coated sample in 3.5 wt.% NaCl

3.7 ANN Modelling of Test Data

Corrosion test data obtained from 80 experimental runs were successfully modelled using ANN with minimal errors (Appendix 1). 56 cases corresponding to 70% of test data were used for training the network and 24 cases corresponding to 30% of test data was used for testing the efficacy of the network. The ANN model was statistically significant with Mean Absolute Error of 0.7803 and 2.2058 for corrosion rate and inhibition efficiency respectively while the Mean Square Error (MSE) was 2.5460 and 10.4478 for corrosion rate and inhibition efficiency respectively. The model had sum of squares error and average overall relative error of 0.981 and 0.018 respectively for the training component and values of 3.190 and 0.043 for the sum of squares error and average overall relative error respectively for the testing component (figure 12). The parameter estimates are illustrated in figure 13. ANN modelling of corrosion test data revealed that inhibitor concentration had a normalized importance contribution coefficient to the corrosion rate and inhibition efficiency of 0.177 corresponding to 30.4% while exposure time played a more significant role with a normalized importance contribution coefficient to the corrosion rate and inhibition efficiency of 0.583 corresponding to 100% whereas temperature had a normalized importance contribution coefficient to the corrosion rate and inhibition efficiency of 0.240 corresponding to 41.1%. ANN modelling of test data showed very high correlation between obtained experimental data and predicted values by ANN with little residuals and deviation as illustrated in figures 14 and 15.

Model Summary

Training	Sum of Squares Error		.981
	Average Overall Relative Error		.018
	Relative Error for Scale Dependents	CR	.012
		IE	.023
	Stopping Rule Used		1 consecutive step(s) with no decrease in error[a]
	Training Time		0:00:00.01
Testing	Sum of Squares Error		3.190
	Average Overall Relative Error		.043
	Relative Error for Scale Dependents	CR	.040
		IE	.055

a. Error computations are based on the testing sample.

Figure 12: ANN Model summary

Parameter Estimates

		Predicted			
		Hidden Layer 1		Output Layer	
Predictor		H(1:1)	H(1:2)	IE	CR
Input Layer	(Bias)	-.793	-.646		
	[InhConc=.00]	.543	.857		
	[InhConc=1.00]	.115	.516		
	[InhConc=2.00]	-.487	-.414		
	[InhConc=3.00]	-.144	.298		
	[InhConc=5.00]	-1.303	-1.913		
	[Time=5.00]	.476	.279		
	[Time=24.00]	-.732	2.147		
	[Time=120.00]	-.328	.533		
	[Time=240.00]	-.176	.123		
	[Time=360.00]	-.199	-.160		
	[Time=480.00]	-.141	-.276		
	[Time=600.00]	-.024	-.283		
	[Time=720.00]	-.032	-.408		
	[Time=840.00]	.106	-.405		
	[Time=960.00]	.102	-.453		
	[Time=1080.00]	-.014	-.510		
	[Time=1200.00]	.273	-.492		
	[Time=1320.00]	.205	-.478		
	[Time=1440.00]	.246	-.445		
	[Temp=25.00]	-1.002	-1.334		
	[Temp=30.00]	.353	-.255		
	[Temp=40.00]	.262	-.391		
	[Temp=60.00]	.341	-.212		
Hidden Layer 1	(Bias)			-2.015	1.642
	H(1:1)			-2.736	-2.152
	H(1:2)			.199	4.158

Figure 13: Parameter estimates for ANN Model

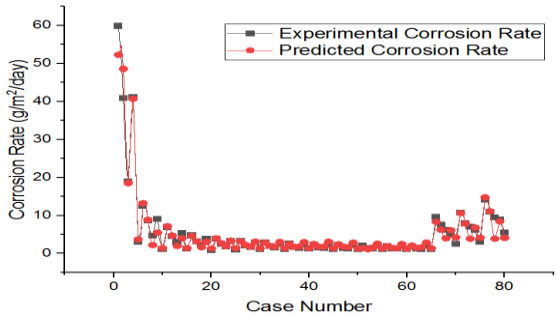

Fig 14: experimental and predicted corrosion rates

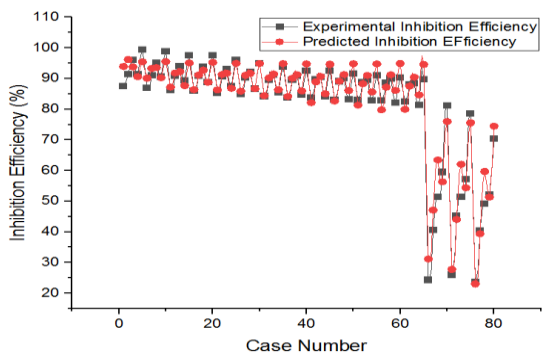

Figure 15: experimental and predicted Inhibition Efficiencies

4 CONCLUSION

1. The synthesis of NiO nanoparticles via chemical precipitation technique with average crystallite size of 23 nm was confirmed by X-ray Diffraction (XRD) and Energy Dispersive X-ray Analysis (EDX).

2. The corrosion rate of mild steel in 3.5 wt. % NaCl generally decreased with increasing exposure time and increasing inhibitor concentration but increased with rise in temperature.

3. The maximum inhibition efficiency of 99.4% was obtained after 24 hours for inhibitor concentration of 5.0 wt. % NiO in epoxy resin at a temperature of 25oC while the corrosion rate reduced from 59.86 to 3.07g/m2/day.

4. Surface Roughness values from Atomic Force Microscopy (AFM) of epoxy coatings containing NiO nanoparticles were significantly lower than the pure epoxy-coated and blank steel samples in 3.5 wt. % NaCl.

5. Values for corrosion rate and percentage inhibition efficiency obtained from experiments were close to the corresponding values predicted by the Artificial Neural Network (ANN) model.

6. The ANN model was statistically significant with Mean Absolute Error of 0.7803 and 2.2058 for corrosion rate and inhibition efficiency respectively while the Mean Square Error (MSE) was 2.5460 and 10.4478 for corrosion rate and inhibition efficiency respectively. The model had sum of squares error of 0.981, average overall relative error of 0.018 for the training component and values of 3.190 and 0.043 for the sum of squares error and average overall relative error respectively for the testing component.

7. The ANN model revealed that the independent variable importance was of the order Exposure Time > Temperature > Inhibitor Concentration with coefficients of 0.177, 0.583 and 0.240 for inhibitor concentration, exposure time and temperature respectively.

5 ACKNOWLEDGEMENTS

The authors are grateful to the Africa Centre of Excellence in Future Energies and Electrochemical Systems, Federal University of Technology, Owerri, Imo State, Nigeria for providing the facilities and enabling environment to carry out this work. Support from the World Bank Africa Centers of Excellence for Impact (Ace Impact) project (NUC/ES/507/1/304) is greatly acknowledged.

6 CONFLICT OF INTEREST

The authors declare that there are no conflicts of interest.

7 REFERENCES

[1] R. O. Medupin, K. Ukoba, K. O. Yoro, and T.-C. Jen, "Sustainable approach for corrosion control in mild steel using plant-based inhibitors: A review," Mater. Today Sustain., vol. 22, p. 100373, 2023, doi: 10.1016/j.mtsust.2023.100373.

[2] Q. Wang, Z. Fan, B. Du, L. Zong, C. Mi, and Y. Wu, "Outline Design of an Atmospheric Corrosion Data Monitoring System," E3S Web Conf., vol. 478, 2024, doi: 10.1051/e3sconf/202447801028.

[3] G. K. P. Barboza, M. C. C. de Oliveira, M. A. Neves, and A. Echevarria, "Justicia brandegeeana as a green corrosion inhibitor for carbon steel in sulfuric acid," Green Chem. Lett. Rev., vol. 17, no. 1, 2024, doi: 10.1080/17518253.2024.2320254.

[4] G. Z. Moldabayeva, A. L. Kozlovskiy, E. I. Kuldeyev, A. K. Syzdykov, and N. S. Buktukov, "Efficiency of using nitride and oxy-nitride coatings for protection against high-temperature oxidation and embrittlement of the surface layer of steel structures," ES Mater. Manuf., pp. 1–10, 2024, doi: 10.30919/esmm1129.

[5] S. U. Nwigwe, R. Umunakwe, S. O. Mbam, M. Yibowei, K. Okon, and G. Kalu-Uka, "The inhibition of Carica papaya leaves extract on the corrosion of cold worked and annealed mild steel in HCl and NaOH solutions using a weight loss technique," Eng. Appl. Sci. Res., vol. 46, no. 2, pp. 114–119, 2019, doi: 10.14456/easr.2019.14.

[6] M. D. R. S. Campos, C. Blawert, N. Scharnagl, M. Störmer, and M. L. Zheludkevich, "Cathodic Protection of Mild Steel Using Aluminium-Based Alloys," Materials (Basel)., vol. 15, no. 4, 2022, doi: 10.3390/ma15041301.

[7] A. C. Emmanuel and G. C. Udeokpote, "Ethanol Extract of Vernonia amygdalina Leaf as a Green Corrosion Inhibitor for Carbon Steel in Solution of HCl," Commun. Phys. Sci., vol. 10, no. 3, pp. 182–193, 2024.

[8] A. I. Ndukwe, N. E. Dan, J. U. Anaele, C. C. Ozoh, K. Okon, and P. C. Agu, "The inhibition of mild steel corrosion by papaya and neem extracts," Mater. Prot., vol. 64, no. 3, pp. 274–282, 2023, doi: 10.5937/zasmat2303274N.

[9] O. Dagdag et al., "Epoxy resin and TiO2 composite as anticorrosive material for carbon steel in 3 % NaCl medium : Experimental and computational studies," J. Mol. Liq., vol. 317, pp. 1–8, 2020, doi: 10.1016/j.molliq.2020.114249.

[10] V. P. M. Shajudheen, K. A. Rani, V. S. Kumar, A. U. Maheswari, M. Sivakumar, and S. S. Kumar, "Comparison of Anticorrosion Studies of Titanium Dioxide andNickel Oxide Thin Films Fabricated by Spray Coating Technique," Mater. Today Proc., vol. 5, no. 2, pp. 8889–8898, 2018, doi: 10.1016/j.matpr.2017.12.322.

[11] R. H. Al-dahiri, A. M. Turkustani, and M. A. Salam, "The Application of Zinc Oxide Nanoparticles as An Eco- Friendly Inhibitor for Steel in Acidic Solution," Int. J. Electrochem. Sci., vol. 15, pp. 442–457, 2020, doi: 10.20964/2020.01.01.

[12] A. M. Atta and H. A. Al-lohedan, "Corrosion Inhibition Efficiency of Modified Silver Nanoparticles For Carbon Steel in 1 M HCl," Int. J. Electrocchemical Sci., vol. 8, pp. 4873–4885, 2013.

[13] M. Perachiselvi, J. Jenson, M. Sakthi, and T. A. Feiona, "FABRICATION OF NICKEL OXIDE NANOPARTICLES FOR ANTIBACTERIAL AND PHOTOCATALYTIC ACTIVITY," Res. J. Life Sci. Bioinformatics, Pharm. Chem. Sci., vol. 4, no. 749, pp. 749–760, 2018, doi: 10.26479/2018.0406.59.

[14] H. M. K. Sheit, M. S. Mubarak, M. M. Varusai, and M. Jaaprasadh, "Enhanced Anti-Corrosion Efficiency and Antimicrobial Properties of Green Synthesised Nickel Oxide (NiO) Nanoparticles," Res. Sq., pp. 1–27, 2023.

[15] V. M. Shajudheen, V. S. Kumar, A. U. Maheswari, M. Sivakumar, S. S. Kumar, and K. A. Rani, "Characterization and anticorrosion studies of spray coated nickel oxide (NiO) thin films," Mater. Today Proc., vol. 5, no. 2, pp. 8577–8586, 2018, doi: 10.1016/j.matpr.2017.11.555.

[16] J. R. Xavier, "Electrochemical, mechanical and adhesive properties of surface modified NiO-epoxy nanocomposite coatings on mild steel," Mater. Sci. Eng. B, vol. 260, no. July, p. 114639, 2020, doi: 10.1016/j.mseb.2020.114639.

[17] M. Ibrahim, K. Kannan, H. Parangusan, S. Eldeib, and O. Shehata, "Enhanced Corrosion Protection of Epoxy / ZnO-NiO Nanocomposite Coatings on Steel," Coatings, vol. 10, no. 783, pp. 1–14, 2020.

[18] A. Ghosal, S. Iqbal, and S. Ahmad, "NiO nano fi ller dispersed hybrid Soy epoxy anticorrosive coatings," Prog. Org. Coatings, vol. 133, no. April, pp. 61–76, 2019, doi: 10.1016/j.porgcoat.2019.04.029.

[19] Z. T. Khodair, A. A. Khadom, and H. A. Jasim, "Corrosion protection of mild steel in

different aqueous media via epoxy / nanomaterial coating : preparation , characterization and mathematical views," J. Mater. Res. Technol., no. x x, pp. 1–12, 2018, doi: 10.1016/j.jmrt.2018.03.003.

[20] C. N. Anyakwo and A. I. Ndukwe, "Prognostic Model for Corrosion-Inhibition of Mild Steel in Hydrochloric Acid by Crushed Leaves of Voacanga Africana," Int. J. Comput. Theor. Chem., vol. 5, no. 3, pp. 30–41, 2017, doi: 10.11648/j.ijctc.20170503.12.

[21] A. I. Ndukwe and C. N. Anyakwo, "Modelling of Corrosion Inhibition of Mild Steel in Hydrochloric Acid by Crushed Leaves of Sida Acuta (Malvaceae)," Int. J. Eng. Sci., pp. 22–33, 2017.

[22] M. Mohammad, A. Irfan, and S. Mohd, "Investigation into the highly efficient Artemisia absinthium -silver nanoparticles composite as a novel environmentally benign corrosion inhibitor for mild steel in 1M HCl," J. Adhes. Sci. Technol., vol. 0, no. 0, pp. 1–26, 2022, doi: 10.1080/01694243.2022.2075523.

[23] C. A. Ramírez-Herrera, I. Cruz-Cruz, I. H. Jiménez-Cedeño, O. Martínez-Romero, and A. Elías-Zúñiga, "Influence of the epoxy resin process parameters on the mechanical properties of produced bidirectional [±45◦] carbon/epoxy woven composites," Polymers (Basel)., vol. 13, no. 8, 2021, doi: 10.3390/polym13081273.

[24] M. Pannico, G. Mensitieri, and P. Musto, "In-situ FTIR spectroscopy of epoxy resin degradation: kinetics and mechanisms," Front. Chem., vol. 12, no. October, pp. 1–14, 2024, doi: 10.3389/fchem.2024.1476965.

[25] Z. Hao, W. Zhang, W. Chen, P. Mei, and L. Lai, "Relationship between the molecular structure of different dithiocarbamates and their oil removal performance," Water Sci. Technol., vol. 86, no. 3, pp. 467–481, 2022, doi: 10.2166/wst.2022.221.

[26] M. S. Alshammari, "Tetraethylenepentamine-Grafted Amino Terephthalic Acid-Modified Activated Carbon as a Novel Adsorbent for Efficient Removal of Toxic Pb(II) from Water," Molecules, vol. 29, no. 7, 2024, doi: 10.3390/molecules29071586.

[27] A. Rahdar, M. Aliahmad, and Y. Azizi, "NiO Nanoparticles: Synthesis and Characterization," J. Nanostructures, vol. 5, pp. 145–151, 2015.

[28] A. A. Ayoola, O. S. I. Fayomi, O. Agboola, B. M. Durodola, A. O. Adegbite, and A. A. Etoroma, "Thermodynamic and Adsorption Influence on the Corrosion Inhibitive Performance of Pawpaw Seed on A36 Mild Steel in 1 M H2SO4 Medium," J. Bio- Tribo-Corrosion, vol. 7, no. 3, pp. 1–12, 2021, doi: 10.1007/s40735-021-00555-y.

[29] R. Hsissou, A. Bekhtaa, A. Elharfia, B. Benzidia, and N. Hajjajib, "Theoretical and electrochemical studies of the coating behavior of a new epoxy polymer: Hexaglycidyl ethylene of methylene dianiline (HGEMDA) on E24 steel in 3.5% NaCl," Port. Electrochim. Acta, vol. 36, no. 2, pp. 101–117, 2018, doi: 10.4152/pea.201802101.

[30] H. Hassannejad and A. Nouri, "Sun flower seed hull extract as a novel green corrosion inhibitor for mild steel in HCl solution," J. Mol. Liq., vol. 254, pp. 377–382, 2018, doi: 10.1016/j.molliq.2018.01.142.

Appendix 1: Summary of Corrosion Rate and Inhibition Efficiency data modelled by ANN

Case No.	Inhibitor Conc. (wt. % NiO)	Time (hours)	Temp. (oC)	Experimental Corrosion Rate (g/m2/day)	Experimental Inhibition Efficiency (%)	Predicted CR (g/m2/day)	Predicted IE (%)	Error in Prediction (CR)	Error in Prediction (I.E.)
1	0	24	25	59.86	87.42	52.29	93.92	7.57	-6.5
2	1	24	25	40.86	91.42	48.58	96.18	-7.72	-4.76
3	2	24	25	18.93	96.02	18.55	93.8	0.38	2.22
4	3	24	25	41.07	91.37	40.72	90.63	0.35	0.74
5	5	24	25	3.07	99.4	3.67	95.44	-0.6	3.96
6	0	120	25	12.54	87	13.22	90.13	-0.68	-3.13
7	1	120	25	8.69	90.99	8.84	93.31	-0.15	-2.32

8	2	120	25	4.69	95.14	2.2	93.57	2.49	1.57
9	3	120	25	9.09	90.56	5.5	90.27	3.59	0.29
10	5	120	25	1.09	98.87	1.36	95.5	-0.27	3.37
11	0	240	25	6.91	86.26	7.15	87.2	-0.24	-0.94
12	1	240	25	4.57	90.91	4.7	91.8	-0.13	-0.89
13	2	240	25	2.99	94.05	1.98	92.23	1.01	1.82
14	3	240	25	5.37	89.32	4.02	87.67	1.35	1.65
15	5	240	25	1.24	97.53	1.38	95.09	-0.14	2.44
16	0	360	25	4.73	86.04	4.6	86.36	0.13	-0.32
17	1	360	25	3.1	90.85	3.15	91.13	-0.05	-0.28
18	2	360	25	2.12	93.74	1.62	92.75	0.5	0.99
19	3	360	25	3.8	88.79	3.07	88.75	0.73	0.04
20	5	360	25	0.84	97.52	1.29	95.28	-0.45	2.24
21	0	480	25	3.79	85.35	3.99	86.29	-0.2	-0.94
22	1	480	25	2.42	90.65	2.7	91.33	-0.28	-0.68
23	2	480	25	1.8	93.04	1.87	91.76	-0.07	1.28
24	3	480	25	3.22	87.56	3.31	86.82	-0.09	0.74
25	5	480	25	1.03	96.02	1.38	94.94	-0.35	1.08
26	0	600	25	3.22	84.8	3.21	85.87	0.01	-1.07
27	1	600	25	2.06	90.27	2.23	91.08	-0.17	-0.81
28	2	600	25	1.66	92.16	1.82	91.7	-0.16	0.46
29	3	600	25	2.83	86.64	3.11	86.7	-0.28	-0.06
30	5	600	25	1.08	94.9	1.38	94.92	-0.3	-0.02
31	0	720	25	2.85	84.22	2.83	84.4	0.02	-0.18
32	1	720	25	1.89	89.53	2	90.2	-0.11	-0.67
33	2	720	25	1.58	91.25	1.75	91.46	-0.17	-0.21
34	3	720	25	2.63	85.44	3.01	86.31	-0.38	-0.87
35	5	720	25	1.1	93.91	1.36	94.86	-0.26	-0.95
36	0	840	25	2.57	83.73	2.43	84.15	0.14	-0.42
37	1	840	25	1.66	89.49	1.75	90.09	-0.09	-0.6
38	2	840	25	1.44	90.89	1.77	91.25	-0.33	-0.36
39	3	840	25	2.43	84.62	2.98	85.94	-0.55	-1.32
40	5	840	25	1.18	92.53	1.37	94.79	-0.19	-2.26
41	0	960	25	2.3	83.77	2.48	82.16	-0.18	1.61
42	1	960	25	1.47	89.62	1.77	88.93	-0.3	0.69
43	2	960	25	1.36	90.4	1.77	90.69	-0.41	-0.29
44	3	960	25	2.24	84.19	3.06	85.02	-0.82	-0.83
45	5	960	25	1.07	92.45	1.37	94.63	-0.3	-2.18
46	0	1080	25	2.16	83.1	2.4	82.66	-0.24	0.44

47	1	1080	25	1.4	89.05	1.75	89.11	-0.35	-0.06
48	2	1080	25	1.26	90.14	1.63	91.29	-0.37	-1.15
49	3	1080	25	2.14	83.25	2.84	86.07	-0.7	-2.82
50	5	1080	25	1.07	91.63	1.32	94.84	-0.25	-3.21
51	0	1200	25	1.99	82.93	1.4	81.32	0.59	1.61
52	1	1200	25	1.31	88.77	1.13	88.3	0.18	0.47
53	2	1200	25	1.22	89.53	1.54	91.01	-0.32	-1.48
54	3	1200	25	2	82.85	2.6	85.59	-0.6	-2.74
55	5	1200	25	1.04	91.08	1.31	94.76	-0.27	-3.68
56	0	1320	25	1.88	82.8	1.9	79.79	-0.02	3.01
57	1	1320	25	1.24	88.66	1.45	87.18	-0.21	1.48
58	2	1320	25	1.21	89.93	1.35	91.24	-0.14	-1.31
59	3	1320	25	1.96	82.07	2.49	86.14	-0.53	-4.07
60	5	1320	25	1.06	90.3	1.24	94.88	-0.18	-4.58
61	0	1440	25	1.78	82.46	2.07	79.95	-0.29	2.51
62	1	1440	25	1.21	88.07	1.52	87.52	-0.31	0.55
63	2	1440	25	1.17	88.47	1.62	90.46	-0.45	-1.99
64	3	1440	25	1.89	81.38	2.87	84.66	-0.98	-3.28
65	5	1440	25	1.04	89.75	1.33	94.59	-0.29	-4.84
66	0	5	30	9.6	24.29	8.35	31.15	1.25	-6.86
67	1	5	30	7.54	40.54	6.26	47.09	1.28	-6.55
68	2	5	30	6.17	51.34	3.97	63.43	2.2	-12.09
69	3	5	30	5.14	59.46	6.12	56.32	-0.98	3.14
70	5	5	30	2.4	81.07	4.21	76	-1.81	5.07
71	0	5	40	10.66	25.97	10.61	27.76	0.05	-1.79
72	1	5	40	7.88	45.27	7.83	44.06	0.05	1.21
73	2	5	40	7	51.39	3.85	62.04	3.15	-10.65
74	3	5	40	6.17	57.15	6.8	54.36	-0.63	2.79
75	5	5	40	3.09	78.54	4.13	75.59	-1.04	2.95
76	0	5	60	14.15	23.55	14.76	23.01	-0.61	0.54
77	1	5	60	11.02	40.46	11.11	39.39	-0.09	1.07
78	2	5	60	9.4	49.22	3.87	59.69	5.53	-10.47
79	3	5	60	8.85	52.19	8.44	51.32	0.41	0.87
80	5	5	60	5.48	70.39	4.1	74.47	1.38	-4.08